# Vacuum-UV negative photoion spectroscopy of CH4

Nicola J Rogers, Matthew James Simpson, Richard P Tuckett, Ken F Dunn, Colin J Latimer

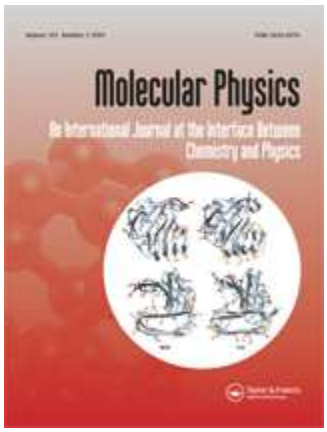


# Vacuum-UV negative photoion spectroscopy of CH4

| | |
|---|---|
| Journal: | *Molecular Physics* |
| Manuscript ID: | TMPH-2009-0329.R1 |
| Manuscript Type: | Special Issue Paper - In honour of Prof Richard Zare |
| Date Submitted by the Author: | 27-Nov-2009 |
| Complete List of Authors: | Rogers, Nicola; University of Birmingham, Chemistry<br>Simpson, Matthew; University of Birmingham, Chemistry<br>Tuckett, Richard; The University of Birmingham, School of Chemistry<br>Dunn, Ken; Queens University Belfast, Physics<br>Latimer, Colin; Queens University Belfast, Physics |
| Keywords: | methane, ion-pair formation, vacuum-UV, absolute cross sections, quantum yields |
| | |

(Reference TMPH-2009-0329) Revised copy submitted electronically to *Mol. Phys.* 27.11.09

**Changes in Red and Bold**

# Vacuum-UV negative photoion spectroscopy of $CH_4$ #

N. J. Rogers [1], M. J. Simpson [1], R. P. Tuckett [1,*], K. F. Dunn [2], C. J. Latimer [2]

1. *School of Chemistry, University of Birmingham, Edgbaston, Birmingham, B15 2TT, UK.*
2. *Department of Physics and Astronomy, Queen's University Belfast, Belfast BT7 1NN, UK.*

No. of pages: 15 (including references, but excluding figures, captions and tables)

No. of figures: 4

No. of tables: 3

# To celebrate the career and multiple birthdays of Professor Dick Zare

* Author for correspondence: (fax) +44 121 414 4403 (email) r.p.tuckett@bham.ac.uk

---

Using synchrotron radiation in the range 12–35 eV, negative ions are detected by mass spectrometry following vacuum-UV photoexcitation of methane. Ion yields for $H^-$, $CH^-$ and $CH_2^-$ are recorded, the spectra of $CH^-$ and $CH_2^-$ for the first time. All ions display a linear dependence of signal with pressure, showing that they arise from unimolecular ion-pair dissociation. Cross sections for ion-pair formation are put onto an absolute scale by calibrating the signal strengths with those of $F^-$ from $SF_6$ and $CF_4$. Following normalisation to total vacuum-UV absorption cross sections, quantum yields for anion production are reported. There is a major discrepancy in the $H^-$ cross section with an earlier measurement, which remains unresolved. The anions arise from both direct and indirect ion-pair mechanisms. For a generic polyatomic molecule AB, the former is defined as $AB \rightarrow A^- + B^+$ (+ neutrals), the latter as the predissociative crossing of an initially-excited Rydberg state of AB by an ion-pair state. In a separate experiment, the threshold photoelectron spectrum of the second valence band of $CH_4$, ionisation to $CH_4^+$ $\tilde{A}\ ^2A_1$ at 22.4 eV, is recorded with an instrumental resolution of 0.004 eV; many of the Rydberg states observed in indirect ion-pair formation converge to this state. The widths of the peaks are lifetime limited, increasing with increasing $v$ in the $\nu_1$ ($a_1$) vibrational ladder. They are the first direct measurement of an upper value to the dissociation rate of these levels into fragment ions.

---

Keywords: methane; ion-pair formation; vacuum-UV; absolute cross sections; quantum yields.

## 1. Introduction

The interaction of electromagnetic radiation with the prototypical molecule, methane, is of fundamental interest because it is central to organic chemistry and abundant in our upper atmosphere. Much previous photochemical analysis has therefore been performed on the molecule. Being closed-shell and very stable, the lowest-lying excited electronic states of methane lie at high energies above the ground state, in the vacuum-UV region. As a consequence, much of the atmospheric photochemistry of methane is driven by intense solar atomic emission lines, such as Lyman-α radiation [1,2].

Methane is a tetrahedral molecule with the electron configuration: $(1a_1)^2(2a_1)^2(1t_2)^6$ , and photoionisation has been studied by He I and He II Photoelectron spectroscopy [3-9]. The removal of the $1t_2$ electron, at *ca.* 13 eV, is known to give rise to the triply-degenerate ground state of $CH_4^+$ , and much detailed work has been carried out to study the nature of the Jahn-Teller distortion of the cation from tetrahedral symmetry [4,10,11]. The $(2a_1)^{-1}$ band at *ca.* 22 eV gives rise to a long vibrational progression in the $\nu_1$ ($a_1$) mode [8], and the $(1a_1)^{-1}$core excitation at *ca.* 290 eV has been studied with vibrational resolution, revealing a shorter $\nu_1$ vibrational progression, reviewed in [12]. Recent experimental studies have been undertaken to investigate the non-Franck-Condon behaviour of this core photoexcitation [13,14]. Between the $(2a_1)^{-1}$ and the $(1a_1)^{-1}$ ionisation energies (IEs), weak satellite peaks have been observed in the photoelectron spectrum, which have been assigned as 'double-hole one-electron' states of $CH_4^+$ [8]. The formation of doubly-excited states of methane by photoexcitation, which correspond to Rydberg states that converge on these satellite states of $CH_4^+$ , have been investigated by dispersed fluorescence [15,16].

There have been many studies of the dissociation products following ionisation of $CH_4$, revealing the fragmentation dynamics of an energy-selected $CH_4^+$ cation [7,9,17-19], and detailed Lyman-α photofragmentation studies have also been undertaken [2,20]. Total photoabsorption cross sections have been measured in the vacuum-UV range of 10-30 eV many times [21-25], with cross sections ranging from *ca.* $(1 - 5) \times 10^{-17}$ cm$^2$.

In this paper we describe an experiment to detect anions following vacuum-UV excitation as a means to study the decay dynamics of electronically excited states of $CH_4$ due to ion-pair formation, generically described as $AB \rightarrow A^- + B^+$ (+ neutrals). Absolute cross sections and quantum yields have been evaluated for the anions observed. Photoion-pair formation has been detected for many diatomic and small

polyatomic molecules [26]. Dissociative ion-pair states can be accessed *via* direct ion-pair formation, *i.e.* photoabsorption from the ground state directly to the ion-pair state, or *via* pre-dissociation following photoexcitation to an excited neutral state, often a Rydberg state. For the latter process to occur, the excited state must be formed at an energy greater than or equal to the asymptotic energy for ion-pair formation, *and* significant coupling between the two unperturbed wavefunctions is required [27].

The formation of $H^-$ from $CH_4$ has previously been investigated in the energy range 12–27 eV by Mitsuke *et al.* [28,29]. In this paper, we confirm the $H^-$ efficiency curve features that they detected, and extend the range of detection to higher energy. However, there is a significant difference in our value for the absolute cross section for $H^-$ formation from that quoted by Mitsuke *et al.* We also report the first observation of the $CH^-$ and the $CH_2^-$ anions from vacuum-UV photoexcitation of methane, and present absolute cross sections for formation of these anions.

## 2. Experimental

The ion pair apparatus has been described in detail previously [30]. Briefly, a direct jet of the gas under investigation is injected from a needle which orthogonally bisects the incident photon beam. The crossing point is positioned between two grids along the third Cartesian axis. A potential difference applied across these grids attracts negative ions towards a three-element electrostatic lens for focussing, and into a Hiden Analytical HAL IV triple quadrupole mass spectrometer (QMS) for mass selection. Anion detection is achieved by a channeltron electron multiplier. The apparatus and QMS were connected *via* a 1 mm diameter aperture, and were pumped by separate turbomolecular pumps, backed by a common rotary pump. Differential pumping enhances sensitivity by reducing the number of free electrons and secondary collisions in the QMS. All measurements were performed using vacuum-UV radiation from beamline 3.1 at the UK Daresbury Synchrotron Radiation Source (SRS), using a 1 m focal length Wadsworth monochromator to provide tunable radiation in the range 12–35 eV. These energies are available from the higher energy of two gratings mounted back-to-back in the monochromator [31]. The optimum resolution that can be obtained from this beamline is 0.05 nm, corresponding to *ca.* 0.01 eV at 15 eV. However, to enhance sensitivity, the spectra reported in this paper were recorded at a resolution of 0.25–0.60 nm. A 2 mm diameter, 300 mm long capillary light guide was used to connect the beamline to the experimental apparatus, providing the necessary differential pumping.

The base pressure of the apparatus was *ca.* $10^{-7}$ mbar. The pressure was measured in the main chamber using an ionisation gauge, and the introduction of the sample gas to the system raised the pressure to *ca.*

$10^{-5}$ mbar. The sensitivity of the ionisation gauge to $CH_4$, $SF_6$ and $CF_4$, essential for determination of *absolute* cross sections of anion formation, was calibrated in a separate experiment relative to $N_2$ using a capacitance manometer [32]. Gas samples were obtained from Apollo Scientific with quoted purity of > 99.9 %, and were used without further purification.

Mass spectra were recorded to observe all anions produced from photoabsorption of the sample gas by exposure to white light, *i.e.* the grating is set to zero order to act as a mirror. The mass-to-charge ratio (*m/z*) of each peak in the mass spectrum was then defined, and the ion yield recorded as a function of photon energy. Once the peak positions were determined, the anion signal was recorded as a function of gas pressure over a typical range of *ca.* (0.5 – 5.0) x $10^{-5}$ mbar. Anions displaying a linear dependence with pressure can be attributed to ion-pair formation (*i.e.* $AB \rightarrow A^- + B^+$ (+ neutrals)), whereas those showing a non-linear pressure dependence cannot. The latter are likely to result from the two-step kinetic process of dissociative electron attachment (*i.e.* $AB + h\nu \rightarrow AB^+ + e^-$; $AB + e^- \rightarrow A^- + B$), in which the rate of formation of $A^-$ is proportional to the square of the pressure of AB.

The yields of $H^-$, $CH^-$ and $CH_2^-$ all show a linear dependence with pressure. To determine their absolute cross sections, it is necessary to normalise the signals to the photon flux, the ring current, the gas pressure, the ionisation gauge sensitivity, and the relative mass sensitivity of the QMS to detection of the different anions. As in our previous studies on $SF_5CF_3$ [33] and the $CF_3X$ series [34], we can write that:

$$\sigma(h\nu) = k\left(\frac{SM}{frp}\right) \qquad (1)$$

where *S* is the detected signal normalised to unit time, *f* is the relative photon flux which effectively is a measure of the grating efficiency, *r* is the storage ring current, *p* is the sample gas pressure corrected for ionisation gauge sensitivity, and *M* is the relative mass sensitivity of the QMS. *k* is the normalisation constant. Normalisation to *f*, *r* and *p* is facile, but this is not the case for *M*. An extensive set of experiments was therefore performed to determine *M* as a function of (*m/z*), and is described in Section 2.1.

The normalised signals can then be put on an absolute scale by calibration with the $F^-$ signals measured from $SF_6$ ((7 ±2) x $10^{-21}$ $cm^2$ at 14.3 eV [35]) and from $CF_4$ ((1.25±0.25) x $10^{-21}$ $cm^2$ at 13.9 eV [36]). We note, however, that these cross section values from Mitsuke *et al.* are not strictly absolute, but are obtained indirectly from the signal of $O^-$ produced from $O_2$ at 17.3 eV, for which the absolute cross section is known [37]. Strictly, the values of the normalisation constants, $k$ ($F^-/SF_6$) and $k$ ($F^-/CF_4$), should be equivalent, but in fact they differ by a factor of 1.5. Given the number of corrections made to the anion signals in the two experiments, this discrepancy falls within a reasonable expected experimental uncertainty. The average value of $k$ was then used in Equation (1) to determine the absolute cross sections, σ, with units of $cm^2$, for production of $H^-$, $CH^-$ and $CH_2^-$ from $CH_4$.

### 2.1 Mass Discrimination by the QMS

All quadrupole mass spectrometers exhibit an element of mass discrimination due to fringing fields, with a tendency to transmit heavier ions less efficiently [38]. To correct for this effect, the mass factor, $M$, has been determined by comparing the cation mass spectra of many polyatomic molecules in the QMS, following 70 eV electron impact ionisation, to actual mass spectra published in the electronic NIST database [39]. It is assumed that any mass factors in the data presented in reference [39] have been accommodated. $M$ was calculated as a function of ($m/z$), see Figure 1, and was used to normalise the raw anions signals, as explained above. It can be seen that as ($m/z$) increases, the detection efficiency of the QMS decreases and a higher $M$ value is required to correct this effect.

The zero-blast artefact [37], whereby *all* ions entering the quadrupole mass filter may be transmitted when the applied potentials are set to detect $m/z$ 1, is not important in this $CH_4$ study because the $H^-$ signal is dominant. This effect, however, *is* important in the detection of the weak $H^-$ signal from $CH_3X$ ($X$ = F, Cl, Br), where the spectra show significant contributions from the much stronger $X^-$ ion yields [40].

## 3. Thermochemistry

Our work determines appearance energies at 298 K ($AE_{298}$) for fragment anions from $CH_4$, and these can be compared with calculated thermochemical values. Berkowitz has noted that for many polyatomic molecules, a calculated threshold energy is a lower limit to the experimental $AE_{298}$ value of an anion, when suitable assumptions are made about what the accompanying cation and neutral fragment(s) are [26]. Furthermore, in comparing experimental AE values with calculated $\Delta_r H^o_{298}$ values of appropriate dissociation reactions, we are making two assumptions. Firstly, the dissociated fragments are not initially formed with thermal equilibrium, but rather are produced with conserved translational momentum relative

to the centre of mass. Therefore a well-defined thermodynamic temperature cannot be allocated to the moieties and thermal corrections should be made [41]. Secondly, the effects of entropy have been disregarded, whereas for unimolecular dissociative reactions $\Delta_r G^o_{298}$ is always slightly more negative than $\Delta_r H^o_{298}$ because $\Delta n$ (the stoichiometric difference in the number of gas-phase molecules due to the reaction) and hence $\Delta_r S^o_{298}$ are both positive. Both of these effects are ignored in this study, which is deemed justifiable at the relatively modest resolution of the experiment.

Values for $\Delta_r H^o_{298}$ of relevant ion-pair reactions were calculated using literature values for enthalpies of formation ($\Delta_f H^o_{298}$ in kJ mol$^{-1}$): $CH_4$ = −74.9, H = 218.0 (both Ref. 42); $H^-$ = 145, $CH^-$ = 477, $CH_2^-$ = 327, $H^+$ = 1530, $H_2^+$ = 1488, $CH^+$ = 1619, $CH_2^+$ = 1386 and $CH_3^+$ = 1098 (all Ref. 43).

## 4. Results and Discussion

### 4.1 Ion-Pair Spectra

The ion yields of $H^-$, $CH^-$ and $CH_2^-$ from $CH_4$ in the range 12–35 eV are shown in Figures 2(a) – 2(c), respectively. The resolution is 0.6 nm, corresponding to 0.07 eV at 12 eV and 0.28 eV at 24 eV. The $H^-$ signal is the most intense. Since all three anions show a linear dependence of signal with pressure, it is possible to determine the absolute cross sections for anion production. Using absolute, *total* vacuum-UV absorption cross section data from Au *et al.* [24], quantum yields for anion production can also be determined. Table 1 shows these data for the energies at which the $H^-$, $CH^-$ and $CH_2^-$ anions have maximum intensity; 20.6, 29.3 and 24.9 eV, respectively. A very weak signal was detected at *m/z* 15 ($CH_3^-$), but the signal-to-noise ratio was poor, and the features appeared to mimic those in the $CH_2^-$ spectrum. It is difficult to differentiate weak signals between anions in the QMS that are only one *m/z* unit apart, and this spectrum was therefore discarded. Figure 2(d) shows the vibrationally-resolved threshold photoelectron spectrum (TPES) of the second band of $CH_4$, *i.e.* ionisation to $CH_4^+$ $\tilde{A}\ ^2A_1$, recorded with the imaging photoelectron photoion coincidence (iPEPICO) spectrometer at the Swiss Light Source, Paul Scherrer Institute Villigen, Switzerland [44]. There is no similarity between this spectrum and any of the three anion yields over this energy range. In addition to the pressure test, this is further evidence that the anions are not formed by dissociative electron attachment, but by ion-pair dissociation.

#### 4.1.1 Appearance energies and thermochemical thresholds

The arrows in Figures 2(a)–2(c) show the calculated $\Delta_r H^o_{298}$ values for ion-pair dissociation reactions (2) – (10). (As described earlier, we are not distinguishing a reaction *enthalpy* from a reaction *energy*). They take the following values; 13.66, 18.91, 19.06, 23.58, 21.58, 23.40, 26.10, 19.59 and 22.28 eV.

$$CH_4 \rightarrow H^- + CH_3^+ \quad (2)$$

$$CH_4 \rightarrow H^- + CH_2^+ + H \quad (3)$$

$$CH_4 \rightarrow H^- + CH^+ + H_2 \quad (4)$$

$$CH_4 \rightarrow H^- + CH^+ + 2H \quad (5)$$

$$CH_4 \rightarrow CH^- + H^+ + H_2 \quad (6)$$

$$CH_4 \rightarrow CH^- + H_2^+ + H \quad (7)$$

$$CH_4 \rightarrow CH^- + H^+ + 2H \quad (8)$$

$$CH_4 \rightarrow CH_2^- + H_2^+ \quad (9)$$

$$CH_4 \rightarrow CH_2^- + H^+ + H \quad (10)$$

The thermodynamic thresholds can be used to infer the possible decay channels that give rise to each peak in the spectrum. The $AE_{298}$ of $H^-$ precedes the calculated $\Delta_r H^o_{298}$ value of reaction (2) by *ca.* 0.4 eV. This scientific impossibility could be accounted for by uncertainties in the thermochemistry, and/or by contributions from hotbands. However, it is clear that the first peak in the $H^-$ spectrum at *ca.* 15 eV can only arise from reaction (2). The double peak in the $H^-$ spectrum at *ca.* 21 and 22 eV probably corresponds to either or both decay channels shown in reactions (3) and (4). The third broad peak at *ca.* 28 eV has an approximate onset at *ca.* 23 eV, and may correspond to production of $H^-$ by reaction (5).

The $CH^-$ spectrum shows an onset at 22.5 ± 0.2 eV. A weak shoulder is observed up to *ca.* 27 eV, and a second, more prominent onset is apparent at this energy. The first onset could correspond to reaction (6) or (7), although we believe that the shoulder is probably an artefact of the spectrum, resulting from detection of the $CH_2^-$ anion of comparable intensity which is only 1 *m/z* unit apart from $CH^-$. Thus we propose that the true onset of $CH^-$ formation from $CH_4$ is *ca.* 27 eV. It is difficult to assign this second/true onset to a particular dissociation reaction, as it could correspond to reactions (6), (7) and/or

(8). The displacements of the $\Delta_r H^o_{298}$ values of reactions (6) and (7) from the onset of this peak would be reasonable, due to the formation of a new $H_2$ or $H_2^+$ bond, respectively. An energy barrier resulting from forming these bonds is extremely likely, and thus their thermochemical thresholds would be expected to lie below the experimental onsets. The onset at 22.2 ± 0.2 eV in the $CH_2^-$ yield agrees very closely with the enthalpy of reaction (10), but similarly the peak could correspond to reaction (9), with formation of $H_2^+$.

### 4.1.2 The $H^-$ yield from $CH_4$

We now consider the $H^-$ spectrum (Figure 2(a)) in more detail. The line positions and relative peak intensities agree well with those observed by Mitsuke *et al.* [28,29]. The first peak at *ca.* 15 eV, with onset at 13.3 ± 0.1 eV, has been assigned as a *direct* transition to an ion-pair state which dissociates to into $H^-$ ($^1S$) + $CH_3^+$ ( $\tilde{X}\ ^1A_1$') [28]. We note that this onset lies well above the first adiabatic IE of methane, 12.61 eV [4,5], and well below the second adiabatic IE, 22.39 eV [8]. The $H^-$ peak at 15 eV cannot, therefore, coincide with a Rydberg state of $CH_4$, and its broad shape and slow onset indicate direct ion-pair formation [45].

The region between 19.5–23.5 eV in Figure 2(a) contains fine structure that is shown in more detail in a higher-resolution spectrum (Figure 3). Peak positions are listed in Table 2. These features arise from an *indirect* process, in which an initially-excited Rydberg state predissociates into an ion-pair state. Thus the vacuum-UV radiation is probing the spectroscopic features of the Rydberg states. Vibrational structure is observed in three close-lying Rydberg states, and they have been assigned by Mitsuke *et al.* to the $(2a_1)^{-1}(3p)^1$, $(2a_1)^{-1}(4p)^1$ and $(2a_1)^{-1}(5p)^1$ states [28,29]. These Rydberg states converge on the $\tilde{A}\ ^2A_1$ state of $CH_4^+$, so the vibrational progressions observed should mimic closely any vibrational structure in the second photoelectron band of $CH_4$. When an *n*p Rydberg state is excited, the only allowed fundamental frequency in $T_d$ symmetry is the totally-symmetric $\nu_1$ ($a_1$) C–H stretching mode. We observe a vibrational spacing in the $(2a_1)^{-1}(4p)^1$ Rydberg state, in which the vibrational structure is most clearly resolved, of 0.26 ± 0.02 eV or 2097 ± 160 $cm^{-1}$, to be compared with a value for neutral $CH_4$ of 2917 $cm^{-1}$ [42]. As expected, this matches the $\nu_1$ vibrational spacing of $CH_4^+$ $\tilde{A}\ ^2A_1$ of 0.27 ± 0.01 eV, taken from the threshold photoelectron spectrum of this band (Figure 4, data listed in Table 3).

A Rydberg series of energy levels, $E_n$ , is described by the well-known formula:

$$E_n = IE - \left( \frac{R_H}{(n-\delta)^2} \right) \quad (11)$$

where $R_H$ is the Rydberg constant, $n$ is the principal quantum number of the orbital which runs to infinity upon convergence, and δ is its quantum defect. **δ values for the 3p and 4p states are determined to be 0.62 ± 0.02 and 0.58 ± 0.02, to be compared with values of 0.67 and 0.60 from Mitsuke *et al.* [28].** There is some inconsistency in the literature whether to use the adiabatic or the vertical IE in such Rydberg calculations, and this choice can significantly affect the Rydberg assignments for large values of $n$, near the convergence limit. As the Rydberg formula determines the *electronic* series of states, $E_n$ (Equation (11)) should refer to the $v$"=0 → $v$'=0 transition from the ground state to the Rydberg state, and the *adiabatic* IE should be used in Equation (11). However, it is only possible to do this if vibrational structure is resolved in the spectrum and the transition to $v$'=0 is identifiable. In spectra that consist of many unresolved vibrational modes, it is more appropriate to use the vertical IE, because both the vertical Rydberg and vertical ionisation transitions will occur from $v$"=0 to the same value of $v$'. This makes the valid assumption that the geometry and vibrational spacing of the Rydberg and cation states are similar. **In determining the quantum defects of these Rydberg states of $CH_4$, we have calculated all the $v_R \rightarrow v^+ = v_R$ transitions per Rydberg state, using the vibrationally-resolved term values in Tables 2 and 3. The values for the 3p and 4p Rydberg states given above, 0.62±0.02 and 0.58±0.02, are average values. The quantum defect of the $(2a_1)^{-1}(5p)^1$ Rydberg state has not been determined because the $v$"=0 → $v$'=0 transition is not categorically defined. We note that the same vibrational intensity distribution is not expected for the $H^-$ yield produced by indirect ion-pair formation through the np Rydberg series as a photoelectron spectrum of the $CH_4^+$ $\tilde{A}$ $^2A_1$ state; the former is an indirect two-step process, the latter is a direct one-step process. Indeed, a different intensity distribution is observed in the Rydberg 3p and 4p series (Figures 3 and 4).**

Between 23.5 and 33.0 eV, Figure 2(a) displays an extensive peak which has not previously been observed. This peak lies above the second adiabatic IE (22.39 eV [15]), but well below the next IE, *ca.* 290 eV , which corresponds to the $(1a_1)^{-1}$ core ionisation. Thus, it features in an energy range absent of 'single-hole-one-electron' Rydberg states. In addition, the broad and structureless nature of the peak does provide some tangible evidence for a *direct* ion-pair process, **and it could also result from a shape resonance.** However, it seems more likely that this peak results from *indirect* ion-pair formation,

following predissociation of many close, unresolved 'doubly-excited Rydberg states' that converge to a doubly-excited IE of methane. Doubly-excited states of methane have been observed by dispersed fluorescence in the 25-35 eV energy range by Kato *et al.* [15]. The states converge to the 'double-hole one-electron' states of $CH_4^+$, observed as satellites in the photoelectron spectrum by Carlsson Göthe *et al.* [8]. Doubly-excited states were observed as a broad peak at *ca.* 29 eV in the study of Kato *et al.*, which gave rise to fluorescence from atomic hydrogen. They were assigned as Rydberg states converging on the $(1t_2)^{-2}(3a_1)^1$ state of $CH_4^+$ at 32.1 eV, that produce excited H atoms *via* predissociation [8]. Furthermore, it is possible that the broad peaks in the $CH^-$ and the $CH_2^-$ spectra (Figures 2(b) and 2(c)) at *ca.* 29 and 25 eV, respectively, also arise from indirect ion-pair formation, resulting from *different* ion-pair states crossing these *same* doubly-excited Rydberg states. We note that the signals of $H^-$, $CH^-$ and $CH_2^-$ have all virtually disappeared at 32.1 eV. In addition, reactions (5), (8) and (10), which we believe to be the most likely routes for formation of these three anions at energies above 25 eV, all involve the production of neutral H atoms.

### 4.1.3 Absolute cross sections and quantum yields for anion formation

The absolute cross section for $H^-$ formation, $1.4 \times 10^{-22}$ cm$^2$ at the peak of the $(2a_1)^{-1}(3p)^1$ Rydberg state at 20.6 eV, is a factor of *ca.* 70 smaller than the value quoted by Mitsuke *et al.* at the slightly higher energy of 21.5 eV, the peak of the 4p Rydberg state [29]. Whilst the errors made in evaluating absolute cross sections are often underestimated in the literature, we do not believe that this major discrepancy can be explained by an accumulation of individual errors in the various correction factors described in Section 2. Overall, we believe that our cross sections are accurate to within a factor of 2–3. The corrections made by Mitsuke *et al.* to their signals to determine absolute σ values are not clear, and in particular it is not apparent whether they have applied any mass discrimination correction factor for detection of *m/z* 1 anions in their quadrupole mass spectrometer. We therefore measured the $H^-$ yield from $C_2H_6$ and $C_3H_8$, obtained absolute cross sections in the manner described earlier, and compared our data with that of Mitsuke *et al.* for these larger saturated hydrocarbons [29]. Rather surprisingly, the results are in reasonable agreement [46]. For example, at the energy at which the cross section is a maximum, 18.9 eV, we determine σ ($H^-/C_2H_6$) to be $1.7 \times 10^{-21}$ cm$^2$, to be compared with $2.2 \pm 0.9 \times 10^{-21}$ cm$^2$ from Mitsuke *et al.* For $H^-/C_3H_8$, at the peak energy of 18.7 eV, we determine a cross section of $3.4 \times 10^{-21}$ cm$^2$, to be compared with the value from Mitsuke *et al.* of $1.6 \pm 1.0 \times 10^{-21}$ cm$^2$. It appears, therefore, that the detection of *m/z* 1 anions is not the reason, *per se*, for the anomalously high value for σ ($H^-/CH_4$) of Mitsuke *et al.*

We note that in comparing cross sections for $H^-$ formation from $CH_4$ to $F^-$ formation from $CF_4$, we might expect the $H^-$ cross sections to be smaller on electronegativity grounds because the C–H bonds are polarised $C^{\delta-}$–$H^{\delta+}$, whereas the C–F bonds are polarised $C^{\delta+}$–$F^{\delta-}$ [3]. Assuming that the cross section for $F^-/CF_4$ at 13.9 eV, 1.25 x $10^{-21}$ $cm^2$ [36], is correct, and indeed our data are calibrated to this value (Section 2), then it is surprising that the value of the cross section for $H^-/CH_4$ from Mitsuke *et al.* is eight times greater than that for $F^-/CF_4$, whereas our value is nine times smaller. We have also observed this trend in cross sections (*i.e.* $\sigma(F^-) > \sigma(H^-)$) for larger hydrocarbons and their perfluorinated equivalents; $C_2H_6$ ($C_2F_6$), $C_3H_8$ ($C_3F_8$) and $C_2H_4$ ($C_2F_4$). In each case, in the range 10–25 eV the maximum value of the $F^-$ cross section is a factor of 2–18 times greater than the maximum value for $H^-$ formation [46]. These arguments provide some evidence, and give confidence to our smaller value of $\sigma(H^-/CH_4)$ shown in Figure 2(a).

Using our cross section values and total absorption cross sections from (e,2e) spectroscopy [24], the absolute quantum yields for $H^-$, $CH^-$ and $CH_2^-$ formation can be calculated. They take values in the range 1–5 x $10^{-6}$ (Table 1). These values are of the same order of magniture as those obtained in our earlier studies on $CF_3X$ ($X$ = Cl,Br,I) [34] and $SF_5CF_3$ [33].

### 4.2 Threshold Photoelectron Spectrum of the second band of $CH_4$

The TPES of the second band of $CH_4$, ionisation to $CH_4^+$ $\tilde{A}\ ^2A_1$ (Figure 2(d), expanded in Figure 4), was recorded at the Swiss Light Source, Paul Scherrer Institute Villigen, Switzerland, using an iPEPICO spectrometer [44]. The photon resolution was 0.004 eV and the step size 0.002 eV. A single progression is observed in $\nu_1$, the totally symmetric C–H stretching mode of $a_1$ symmetry, which peaks at $v$=1. This observation is independent of whether peak intensities or areas are measured. This spectrum has been recorded before by several groups [6-9], but never with an experimental resolution as good as 4 meV. Our peak positions and separations (Table 3) are in excellent agreement with those determined by Carlsson Göthe *et al.* from He II photoelectron spectroscopy [8], and we can unambiguously confirm their tentative observation that the linewidth increases as the vibrational quantum number in the $\nu_1$ mode increases. At a resolution of 4 meV, our signal-to-noise ratio is not good enough to determine peak positions or widths for $v \geq 4$, although data up to $v$ = 14 are quoted by Carlsson Göthe *et al.* Since our experimental resolution is much narrower than the peak widths, deconvolution of the experimental resolution is not necessary, and we directly determine full width at half maximum (FWHM) values of 31, 52, 82 and 99 meV for $v$ = 0, 1, 2 and 3, respectively. These values are roughly a factor of two smaller than those

modelled by Carlsson Göthe *et al*., and approximately correspond to the linewidths of the four vibrational levels of $CH_4^+$ $\tilde{A}\ ^2A_1$ ($\nu_1$). We therefore determine lifetimes of 21, 12, 8 and 6 fs, corresponding to dissociation rates of 4.8 x $10^{13}$, 8.3 x $10^{13}$, 1.2 x $10^{14}$ and 1.7 x $10^{14}$ $s^{-1}$, for $v$ = 0, 1, 2 and 3, respectively. We note that the lifetimes are lower limits and the dissociation rates are upper limits, because it is assumed that *all* the peak broadening is due to the lifetime effect. In particular, we have ignored any effects due to instrumental resolution and rotational fine structure. **It seems very unlikely that the broadening is spectroscopic, and not dynamic, in nature, possibly due to unresolved vibrational polyads at higher energy caused by Coriolis and Fermi interactions, because these should be partially resolvable with a photon resolution of 0.004 eV.**

Threshold photoelectron photoion coincidence measurements have shown that the $\tilde{A}\ ^2A_1$ state of $CH_4^+$ dissociates directly, without prior internal conversion to the electronic ground state [7,9]. Internal conversion is slow due to the large Franck Condon gap of over 6 eV between the $\tilde{A}$ and $\tilde{X}$ states. Thus, the $\tilde{A}\ ^2A_1$ state behaves as an isolated state and dissociates non-statistically. The dominant fragment ion produced from the dissociation is $CH_2^+$, the minority ions being $CH^+$ and $CH_3^+$, and the $\tilde{A}\ ^2A_1$ state of $CH_4^+$ correlates directly to $CH_2^+$ in $C_{2v}$ symmetry [47]; it also correlates to $H^+$ (+ $CH_3$) in $C_{3v}$ symmetry, but the $H^+$ signal is negligible in the experiment. Dutuit *et al.* have therefore suggested that the $\tilde{A}\ ^2A_1$ state of $CH_4^+$ dissociates directly to $CH_2^+ + H_2$ [7]. A sequential dissociation, $(CH_4^+)^* \rightarrow (CH_3^+)^* + H \rightarrow CH_2^+ + H + H$, cannot however be ruled out, and from approximate kinetic energy measurements on $CH_2^+$ is the preferred mechanism of Furuya *et al.* [9]. There is some additional evidence for this latter mechanism from the photoelectron spectrum of the $CH_3$ radical [48], where the first excited singlet electronic state of $CH_3^+$ is observed at 16.1 eV, *i.e.* 20.6 eV above the ground state of $CH_4$ [42]. Thus the first step of this two-step mechanism could be non-radiative dissociation of $CH_4^+$ $\tilde{A}\ ^2A_1$ into high vibrational levels of $CH_3^+$ $\tilde{A}\ ^1E'$ which then decomposes to $CH_2^+$. Whichever mechanism is dominant, the data above give the first experimental measurements of upper limits for the dissociation rate producing $CH_2^+$ for the lowest four $\nu_1$ vibrational levels of $CH_4^+$ $\tilde{A}\ ^2A_1$.

## 5. Conclusions

Absolute cross sections and quantum yields for production of $H^-$, $CH^-$ and $CH_2^-$ from $CH_4$ over the energy range 12–35 eV have been determined. The signals of all three ions display a linear dependence with pressure, showing that they arise from an ion-pair mechanism and not from the multi-step process of

dissociative electron attachment. The $CH^-$ and $CH_2^-$ spectra are observed here for the first time. Whilst the relative yield of $H^-$ is very similar to that observed in an earlier study by Mitsuke *et al.* [28,29], our cross section values are a factor of *ca.* 70 smaller than those quoted earlier. This discrepancy remains unresolved. The $H^-$ peaks are attributed to both direct and indirect ion-pair formation, whereas the $CH^-$ and $CH_2^-$ peaks probably arise from an indirect process, caused by ion-pair states crossing with doubly-excited Rydberg states. The threshold photoelectron spectrum of the second band of $CH_4$, ionisation to $CH_4^+$ $\tilde{A}$ $^2A_1$ at 22.40 eV, has been recorded with a resolution of 0.004 eV. The widths of the peaks observed for $v = 0–3$ in the $\nu_1$ vibrational ladder increase with $v$. They are the first direct measurement of a lower limit to the lifetime, and hence an upper limit to the unimolecular dissociation rate of these levels, into fragment ions.



## Acknowledgments

We thank Dr David Shaw (Manager of beamline 3.1) for help with recording the anion spectra at the Daresbury synchrotron source. We thank Drs Andras Bodi and Melanie Johnson (SLS) and Ms Jonelle Harvey (University of Birmingham) for help with recording the TPES of $CH_4$ on beamline X04DB of the Swiss Light Source. The collaboration between the groups in Birmingham and Belfast was partially funded by EPSRC Network Grant No. GR/N26234/01. The STFC and EU are thanked for the provision of beamtime at the Daresbury synchrotron and the Swiss Light Source, respectively.

## References

[1] R. P. Wayne, *Chemistry of Atmospheres*, 3rd edition, (Oxford University Press, New York) 2000.

[2] P. A. Cook, M. N. R. Ashfold, Y-J. Jee, K.-H. Jung, S. Harich and X. Yang, *Phys. Chem. Chem. Phys.,* **3**, 1848 (2001).

[3] C. R. Brundle, M. B. Robin and H. Basch, *J. Chem. Phys.,* **53**, 2196 (1970).

[4] J. W. Rabalais, T. Bergmark, L. O. Werme, L. Karlsson and K. Siegbahn, *Physica Scripta*, **3**, 13 (1971).

[5] A. W. Potts and W. C. Price, *Proc. R. Soc. Lond. A.*, **326**, 165 (1972).

[6] G. Bieri and L. Asbrink, *J. Electron. Spec. and Rel. Phenom.*, **20**, 149 (1980).

[7] O. Dutuit, M. Aït-Kaci, J. Lemaire and M. Richard-Viard, *Physica Scripta,* **T31**, 223 (1990).

[8] M. Carlsson Göthe, B. Wannberg, L. Karlsson, S. Svensson, P. Baltzer. F. T. Chau and M.-Y. Adam, *J. Chem. Phys.,* **94**, 2536 (1991).

[9] K. Furuya, K. Kimura, Y. Sakai, T. Takayanagi and N. Yonekura, *J. Chem. Phys.,***101**, 2720 (1994).

[10] H. J. Wörner, R. van der Veen and F. Merkt, *Phys. Rev. Lett.*, **97**, 173003 (2006).

[11] H. J. Wörner, X. Qian and F. Merkt, *J. Chem. Phys.,* **126**, 144305 (2007).

[12] U. Hergenhahn, *J. Phys. B,* **37**, R89 (2004).

[13] E. Kukk, K. Ueda, U. Hergenhahn, X.-J. Liu, G. Prümper, H. Yoshida, Y. Tamenori, C. Makochekanwa, T. Tanaka, M. Kitajima and H. Tanaka, *Phys. Rev. Lett.*, **95**, 133001 (2005).

[14] K. Ueda, A. Pavlychev, E. Kukk, U. Hergenhahn, H. Yoshida, T. Sunami, F. Tahara, T. Tanaka, M. Kitajima, H. Tanaka, A. De Fanis and Y. Tamenori, *Chem. Phys. Lett.*, **411**, 33 (2005).

[15] M. Kato, K. Kameta, T. Odagiri, N. Kouchi and Y. Hatono, *J. Phys. B,* **35***,* 4383 (2002).

[16] H. Fukuzawa, T. Odagiri, T. Nakazato, M. Murata, H. Miyagi and N. Kouchi, *J. Phys. B*, **38***,* 565 (2005).

[17] T. A. Field and J. H. D. Eland, *J. Electron. Spec. and Rel. Phenom.*, **73**, 209 (1995).

[18] K.-M. Wietzel, M. Malow, G. K. Jarvis, T. Baer, Y. Song and C. Y. Ng, *J. Chem. Phys.,* **111**, 8267 (1999).

[19] C. J. Latimer, R. A. Mackie, A. M. Sands. N. Kouchi and K. F. Dunn, *J. Phys. B*, **32**, 2667 (1999).

[20] A. J. R. Heck, R. N. Zare and D. W. Chandler, *J. Chem. Phys.*, **104**, 4019 (1996).

[21] E. E. Koch and M. Skibowski, *Chem. Phys. Lett.*, **9**, 429 (1971).

[22] C. Backx, G. R. Wright, R. R. Tol and M. J. van der Wiel, *J. Phys. B,* **8**, 3007 (1975).

[23] J. A. R. Samson, G. N. Haddad, T. Masuoka, P. N. Pareek and D. A. L. Kilcoyne, *J. Chem. Phys*., **90**, 6925 (1989).

[24] J. W. Au, G. Cooper, G. R. Burton, T. N. Olney and C. E. Brion, *Chem. Phys.*, **173**, 209 (1993).

[25] K. Kameta, N. Kouchi, M. Ukai and Y. Hatano, *J. Electron. Spec. and Rel. Phenom.*, **123**, 225 (2002).

[26] J. Berkowitz, in *VUV and Soft X-Ray Photoionization,* (eds: U. Becker and D. A. Shirley), Plenum, New York, 1996, p. 263.

[27] A. G. Suits and J. W. Hepburn, *Annu. Rev. Phys. Chem.,* **57**, 431 (2006).

[28] K. Mitsuke, S. Suzuki, T. Imamura and I. Koyano, *J. Chem. Phys.,* **94**, 6003 (1991).

[29] K. Mitsuke, H. Hattori and H. Yoshida, *J. Chem. Phys.,* **99**, 6642 (1993).

[30] C. A. Hunniford, S. W. J. Scully, K. F. Dunn and C. J. Latimer, *J. Phys. B,* **40**, 1225 (2007).

[31] C. R. Howle, S. Ali, R. P. Tuckett, D. A. Shaw and J. B. West, *Nucl. Instrum. Methods Phys. Res. B*, **237**, 656 (2005).

[32] K. F. Dunn, unpublished data.

[33] M. J. Simpson, R. P. Tuckett, K. F. Dunn, C. A. Hunniford, C. J. Latimer and S. W. J. Scully, *J. Chem. Phys*., **128**, 124315 (2008).

[34] M. J. Simpson, R. P. Tuckett, K. F. Dunn, C. A. Hunniford and C. J. Latimer, *J. Chem. Phys.*, **130**, 194302 (2009).

[35] K. Mitsuke, S. Suzuki, T. Imamura and I. Koyano, *J. Chem. Phys.*, **93**, 8717 (1990).

[36] K. Mitsuke, S. Suzuki, T. Imamura and I. Koyano, *J. Chem. Phys.*, **95**, 2398 (1991).

[37] P. M. Dehmer and W. A. Chupka, *J. Chem. Phys.,* **62**, 4525 (1975).

[38] *Quadrupole Mass Spectrometry*, American Vacuum Society Classics, American Institute of Physics, New York, (ed. Peter H Dawson) (1995).

[39] NIST Chemistry Webbook: http://webbook.nist.gov/chemistry/

[40] N. J. Rogers, M. J. Simpson, R. P. Tuckett, K. F. Dunn and C. J. Latimer, *unpublished data.*

[41] J. C. Traeger and R. G. McLoughlin, *J. Am. Chem. Soc.,* **103**, 3647 (1981).

[42] M. W. Chase, *J. Phys. Chem. Ref. Data Monograph,* **9**, 1 (1998).

[43] S. G. Lias, J. E. Bartmess, J. F. Liebman, J. L. Holmes, R. D. Levin and W. G. Mallard, *J. Phys. Chem. Ref. Data Suppl.,* **17** (1988).

[44] A. Bodi, M. Johnson, T. Gerber, Z. Gengeliczki, B. Sztáray and T. Baer, *Rev. Sci. Instr.,* **80**, 034101 (2009).

[45] J. Berkowitz, *Photoabsorption, Photoionization and Photoelectron Spectroscopy,* Academic press (1979).

**[46] M. J. Simpson, *PhD Thesis, University of Birmingham* (2010), in preparation.**

[47] E. F. van Dishoeck, W. J. van der Hart and M. van Hemert, *Chem. Phys.,* **50**, 45 (1980).

[48] J. Dyke, N. Jonathan, E. Lee and A. Morris, *J. Chem. Soc. Faraday Trans. 2.,* **72**, 1385 (1976).

***Table 1.*** $AE_{298}$ values, and absolute cross sections and quantum yields for production of anions from vacuum-UV photodissociation of $CH_4$.

| Anion | $AE_{298}$ / eV [a] | $\sigma_{anion}$ (max) / $cm^2$ [b] | E / eV [c] | $\Phi_{anion}$ [d] |
|---|---|---|---|---|
| $H^-$ | 13.3 ± 0.1 | $1.4 \times 10^{-22}$ | 20.6 | $4.4 \times 10^{-6}$ |
| $CH^-$ | 22.5 ± 0.2 | $5.9 \times 10^{-23}$ | 29.3 | $4.6 \times 10^{-6}$ |
| $CH_2^-$ | 22.2 ± 0.2 | $2.8 \times 10^{-23}$ | 24.9 | $1.3 \times 10^{-6}$ |

[a] Appearance Energy (AE) at 298 K.

[b] Cross section for ion-pair formation at the peak maximum.

[c] Energy of peak maximum, at which $\sigma_{anion}$ (max) and $\Phi_{anion}$ are taken.

[d] Quantum yields for anion formation, $\Phi_{anion}$, calculated from total vacuum-UV absorption cross sections of $CH_4$ taken from Ref. 24.

***Table 2.*** Vibrational progressions observed in the yield of $H^-$ from $CH_4$ (Figure 3).

| $\nu_1$ vibrational state | | Progression (a) | | Progression (b) | | Progression (c) | |
|---|---|---|---|---|---|---|---|
| | | E / eV | (ΔE / eV) | E / eV | (ΔE / eV) | E / eV | (ΔE / eV) |
| $v$ = | 0 | 20.00 | | 21.24 | | 22.06 [a] | |
| | | | (0.28) | | (0.28) | | (0.26) |
| | 1 | 20.28 | | 21.52 | | 22.32 | |
| | | | (0.24) | | (0.24) | | (0.28) |
| | 2 | 20.52 | | 21.76 | | 22.60 | |
| | | | (0.24) | | (0.24) | | |
| | 3 | 20.76 | | 22.00 | | | |
| | | | | | (0.24) | | |
| | 4 | | | 22.24 | | | |

[a] The assignment of this peak to $v$=0 is not definite, so the vibrational numbering of this progression is not certain.

***Table 3.*** Full Width at Half Maximum (FWHM) values for vibrational peaks in the second photoelectron band of $CH_4$, ionisation to $CH_4^+$ $\tilde{A}$ $^2A_1$ (Figure 4).

| $\nu_1$ vibrational state | | E / eV | ($\Delta$E / eV) | FWHM / meV |
|---|---|---|---|---|
| $v$ = | 0 | 22.40 | | 31 ± 3 |
| | | | (0.27) | |
| | 1 | 22.67 | | 52 ± 5 |
| | | | (0.26) | |
| | 2 | 22.93 | | 82 ± 8 |
| | | | (0.25) | |
| | 3 | 23.18 | | 99 ± 10 |

## *Figure Captions*

**Figure 1:** Graph to determine the relative mass sensitivity of the Hiden Analytical HAL IV quadrupole mass spectrometer as a function of (*m/z*). Sample gases included $CF_4$, $SF_6$, $CF_3SF_5$, $CH_3F$, $CH_3Cl$, $CH_3Br$, $CH_2Cl_2$, $CF_2Cl_2$, $CFCl_3$, $C_2F_4$ and *c*-$C_5F_8$. The mass spectrum of each sample was measured with 70 eV electron impact ionisation, and compared with the NIST spectrum [39]. At each (*m/z*) value, the % yield from NIST is divided by the % yield from our spectrum, and the data are normalised to unity at *m/z* 69 (*i.e.* $CF_3^+$). The squares show the data points, the solid line shows the best fit to a third order polynomial.

**Figure 2:** (a)-(c) Cross sections for $H^-$, $CH^-$ and $CH_2^-$ production following vacuum-UV photoexcitation of $CH_4$. Ion yields were measured between 12 and 35 eV with a step size of 0.1 eV and a wavelength resolution of 0.6 nm. Solid arrows show energies of thermochemical thresholds calculated for reactions (2)–(10), respectively. (d) Threshold photoelectron spectrum of $CH_4$ measured at a resolution of 0.004 eV using the imaging photoelectron photoion coincidence spectrometer at the Swiss Light Source [44]. The step size is 0.002 eV.

**Figure 3:** High resolution $H^-$ scan between 19.5 and 23.5 eV. The step size is 0.02 eV and the resolution is 0.25 nm, *ca.* 0.09 eV. The three progressions (a)-(c), have been assigned by Mitsuke *et al.* [28,29] as vibrational progressions in $\nu_1$ ($a_1$) within different Rydberg states converging on the $\tilde{A}\ ^2A_1$ state of $CH_4^+$. Progression (a) has been assigned as the $(2a_1)^{-1}(3p)^1$ Rydberg state, (b) as the $(2a_1)^{-1}(4p)^1$ Rydberg state, and (c) the $(2a_1)^{-1}(5p)^1$ Rydberg state.

**Figure 4:** Expansion of Figure 2(d). Threshold photoelectron spectrum of the second band of $CH_4$, ionisation to $CH_4^+\ \tilde{A}\ ^2A_1$ recorded with a step size of 0.002 eV and a resolution of 0.004 eV.

*Figure 1*

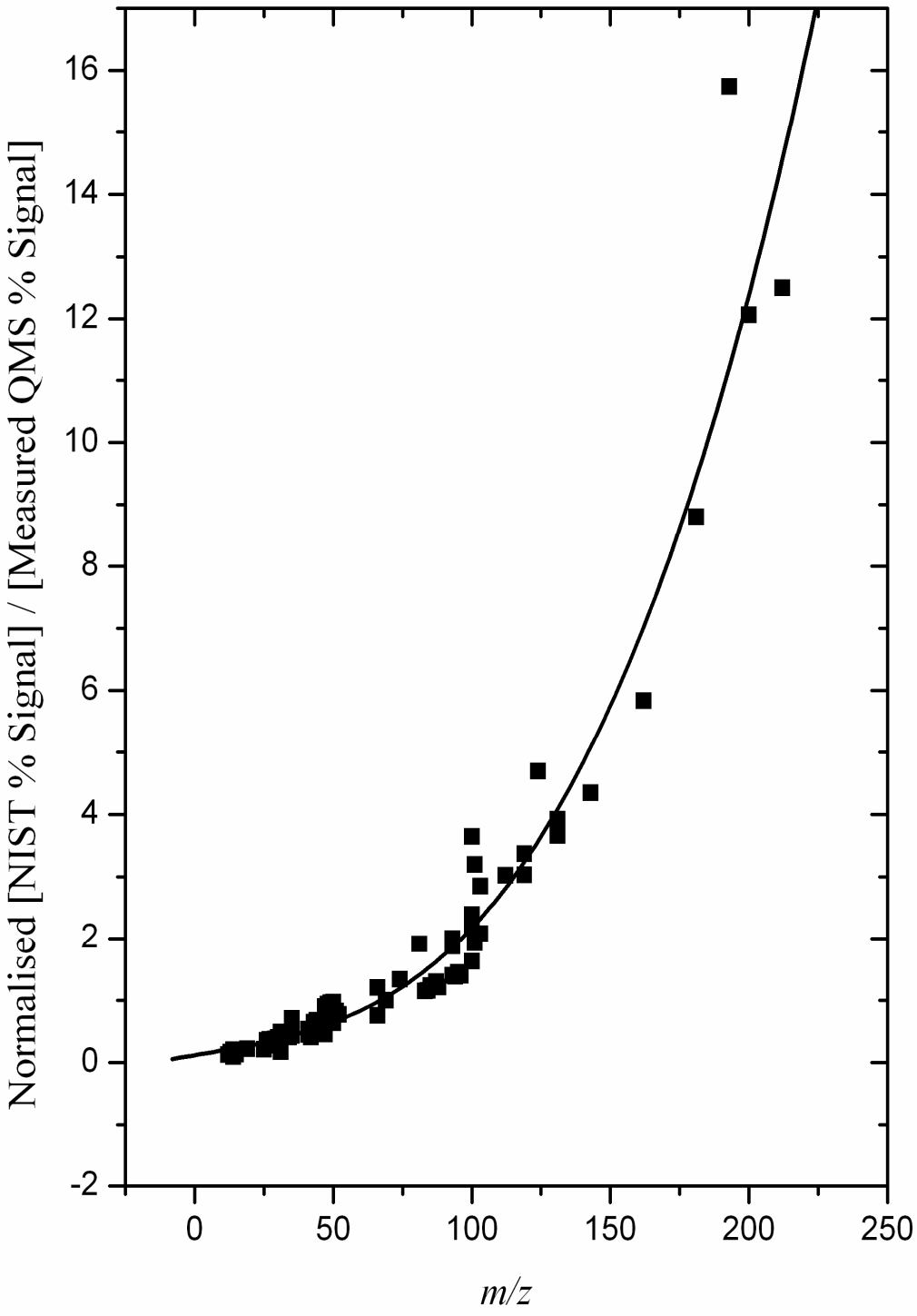
Normalised [NIST % Signal] / [Measured QMS % Signal]
16
14
12
10
8
6
4
2
0
-2
0
50
100
150
200
250
m/z

*Figure 2*

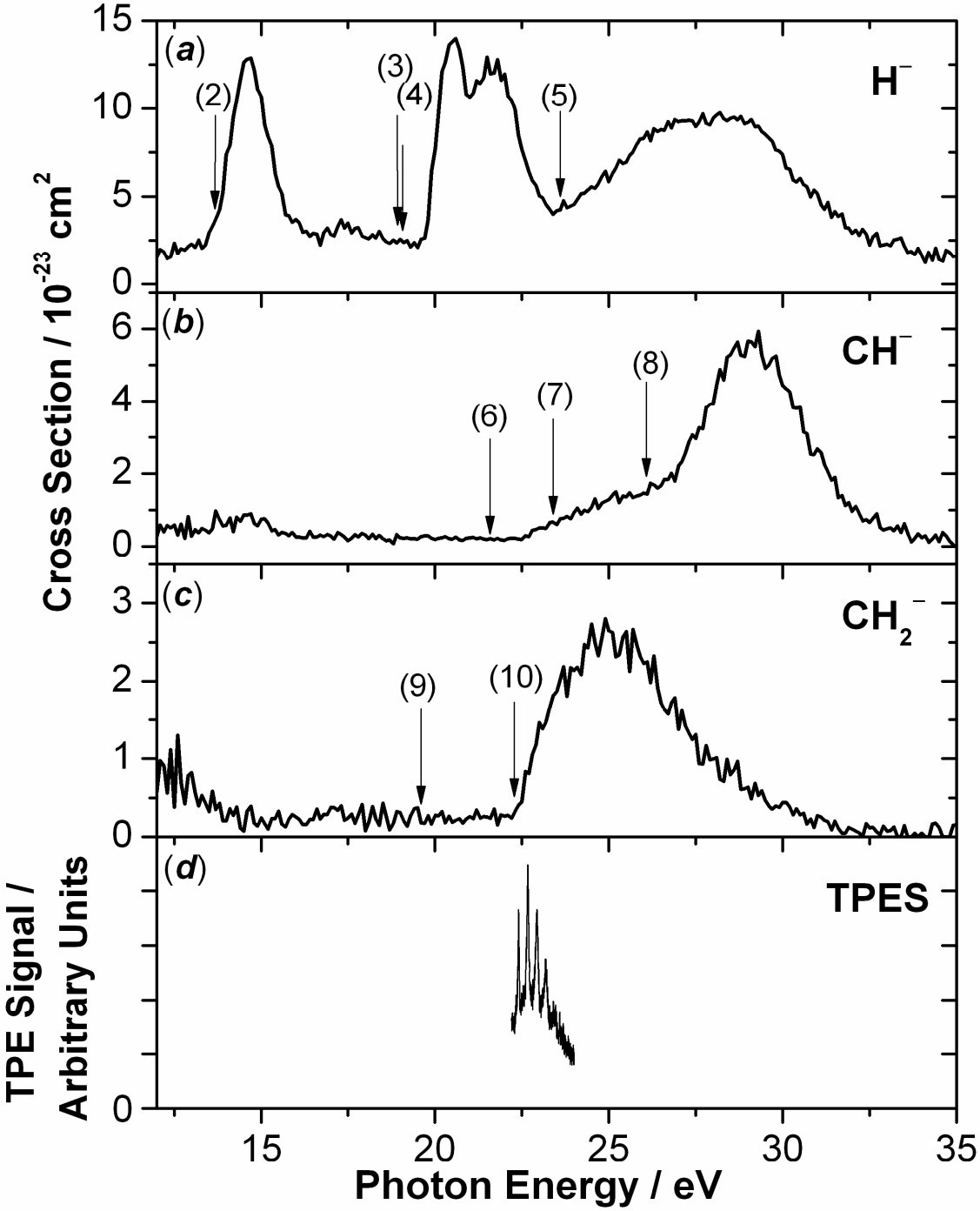
(a)
(2)
(3)
(4)
(5)
H⁻
(b)
(6)
(7)
(8)
CH⁻
(c)
(9)
(10)
CH₂⁻
(d)
TPES
Cross Section / 10⁻²³ cm²
TPE Signal / Arbitrary Units
Photon Energy / eV
0
5
10
15
0
2
4
6
0
1
2
3
0
15
20
25
30
35

*Figure 3*

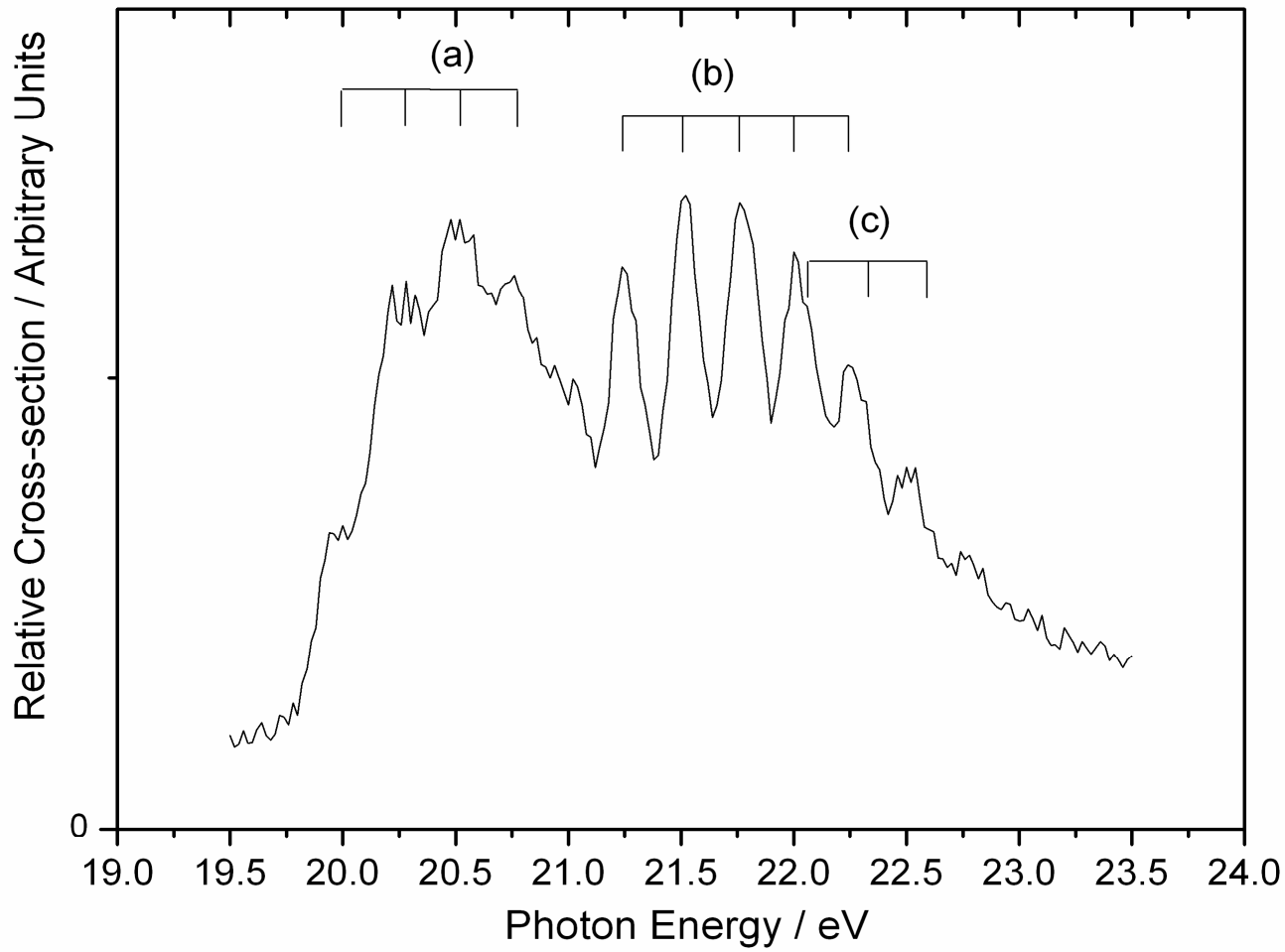

*Figure 4*